Refereed Proceedings

The 12th International Conference on Fluidization - New Horizons in Fluidization Engineering

Engineering Conferences International *Year* 2007

Cold Modelling of an Internally Circulating Fluidized Bed Membrane Reactor

Tony Boyd[*] John R. Grace[†]
C. Jim Lim[‡] A. M. Adris[**]

[*]University of British Columbia, tboyd@membranereactor.com
[†]University of British Columbia, jgrace@chml.ubc.ca
[‡]The University of British Columbia, cjlim@chml.ubc.ca
[**]University of British Columbia

COLD MODELING OF AN INTERNALLY CIRCULATING FLUIDIZED BED MEMBRANE REACTOR

Tony Boyd, John R. Grace, C. Jim Lim, A.M. Adris
Chemical and Biological Engineering, University of British Columbia
2360 East Mall, Vancouver, Canada, V6T 1Z3
T: (604) 822-4343, F: (604) 822-1659, E: tboyd@membranereactor.com

ABSTRACT

A novel fluidized bed membrane reactor with internal catalyst circulation is being developed for the production of high-purity H_2 from an autothermal reformer. In order to provide guidance to pilot reactor testing, a cold model was built to study the influence of reactor configuration on hydrodynamics and catalyst circulation. It was found that catalyst circulation was reproducible, but that parallel non-communicating flow channels could lead to flow instability. Solids circulation was found to be adequate for design of the autothermal reformer.

INTRODUCTION

Steam methane reforming (SMR) is a well-established process which provides the bulk of the world's hydrogen. The process is endothermic. Equilibrium conditions dictate operating temperatures in the range of 800 - 900°C. The net SMR reaction is:

$$CH_4 + 2H_2O \leftrightarrow CO_2 + 4H_2 \qquad \Delta H_{298} = 165 \text{ kJ/mol}$$

If H_2 is removed from the reaction zone with H_2-permeable membranes, the thermodynamic equilibrium is shifted forward, thereby allowing high methane conversions at much lower temperatures (550-650°C) than conventional reformers. The membranes produce a H_2 stream directly from the reactor, which eliminate the need for shift reactors and H_2 purification equipment. Paglieri and Way (1) and Uemiya (2) have reviewed past research on palladium (Pd) membrane reactors applied to the SMR process.

Fluidized beds provide some advantages over conventional fixed bed SMR, including higher catalyst effectiveness and improved heat and mass transfer rates (Adris et al., 3). In this project, a novel internally circulating fluidized bed membrane reactor (ICFBMR) for high-purity H_2 production was developed, patented (Grace et al., 4) and tested in a pilot reactor (Boyd et al., 5). The process couples SMR with planar Pd-alloy H_2-selective membranes (supplied by Membrane Reactor Technologies Ltd.) and direct air addition (autothermal reforming). This reactor configuration has considerable potential for small-scale distributed H_2 production.

Figure 1 presents a schematic of the ICFBMR. Planar, vertical H_2 membranes are separated by gaps within an open-ended draft box. The gas flow pattern within the

The 12th International Conference on Fluidization - New Horizons in Fluidization Engineering, Art. 63 [2007]

fluidized bed induces internal circulation of catalyst particles between the central core (permeation) zone and an outer annulus. Circulating catalyst particles, heated in the oxidation zone, carry the heat required by the endothermic reforming reactions. The main benefits of the internal catalyst circulation are:

- *Temperature uniformity* – The Pd-alloy membranes have a practical operating limit of ~600°C, and hotspots must be avoided. It is also desirable that the membranes be operated at a uniform temperature at optimal design conditions.
- *Heat transfer* – Vigorous particle motion promotes good heat transfer.
- *Separation of air and membranes* – Air should be kept away from the membranes to avoid hotspots.
- *Oxidation air* – Roy (6) demonstrated that O_2 could be added to a bubbling bed reformer. In this study, air was added to the top of the reactor to supply the reforming heat. If the system were well mixed, the N_2 in the air would decrease the H_2 partial pressure in the reactor, reducing the H_2 flux. The ICFBMR system permits the heat of oxidation to be circulated but circulates only a small fraction of the N_2, thus maintaining the H_2 partial pressure in the permeation zone close to those for SMR conditions.

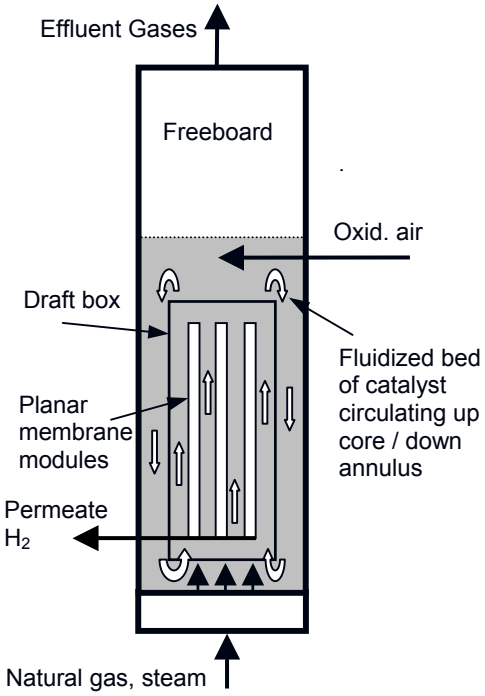

Figure 1: ICFBMR schematic

In order to guide the ICFBMR concept and pilot reactor, cold model experiments were performed in a Plexiglas column with FCC particles and air. The main areas of investigation were:

- Qualitative evaluation of fluidization characteristics.
- Solids circulation as a function of membrane panel and reactor feed rates.
- Evaluation of whether gas from the top air distributor circulates back to the membrane core with the catalyst.

A number of cold model studies have been published on internally circulating fluidized (e.g. Song et al., 7) and spouted (e.g. Milne et al., 8) beds. Most have used an empty circular draft tube to segregate the core and annulus, with solids circulation often restricted by an opening under the draft tube that is much smaller than the cross-sectional area of the draft tube. In contrast, this study used a rectangular draft box filled with vertical plates to mimic hydrogen membrane panels. In addition, the flow access area to the ICFBMR draft box is larger than the flow (open) area in the core. Secondary air addition to the bottom of the annulus was also studied in this work as a possible means of increasing catalyst circulation.

For currently achievable membrane permeation fluxes, the desired superficial gas velocity within the reformer draft box (U_{core}) is between 0.05 and 0.3 m/s. Three

fluidized bed dimensionless scaling parameters proposed by Glickman et al. (9) were matched in this cold model work:

$$\frac{U_{core}^2}{gd_p}, \frac{\rho_p}{\rho_f}, \frac{U_{core}}{U_{mf}} \quad (1)$$

Both the FCC used in the cold model and the ATR catalyst tested in the pilot plant were Geldart type A powders, with a measured U_{mf} in ambient air of ~0.003 m/s. The particle shapes of the two powders were roughly matched. Hydrodynamic data for the cold model and pilot reformer are presented in Table 1, together with values for the three scaling terms, for U_{core} = 0.1 m/s.

Table 1: Pilot reactor and cold model properties and characteristics

Variable	Pilot Plant	Cold Model
Bed material	ATR on alumina	FCC
Particle / gas density (ρ_p, ρ_f, kg/m^3)	2,090 / 2.48	1,600 / 1.20
Average particle diameter (d_p, m)	87E-6	62E-6
Temperature (°C) / pressure (kPa)	600° / 1,200	20° / 101
Fluidization gas	Reformate	Air
Archimedes number	40	15
U_{mf} measured in atmospheric air (m/s)	0.0030	0.0026
Froude number (U^2_{core}/gd_p)	12	16
Density ratio (ρ_p / ρ_f)	842	1,330
Velocity ratio (U_{core} / U_{mf})	56	33

EXPERIMENTAL APPARATUS

Figure 2 presents a schematic of the cold model system. The main section of the column had an inner diameter of 0.285 m. A draft box containing 7 simulated membrane panels was centered in the column. The area of the membrane panels was ~2.9 m^2, corresponding to a permeate H_2 capacity of ~50 Nm^3/h, depending on the type of membrane and reformer operating conditions. There was a 100 mm gap between the main distributor and the bottom of the draft box to return solids from the annulus to the core. FCC solids were added to give a settled bed depth of 25 mm above the top of the core box. An antistatic agent (0.5 wt% of Larostat 519) was added to reduce electrostatic charges.

Air at ambient temperature was metered to the column through three distributors. The main feed was introduced through an orifice plate distributor having 30 - 5.8 mm diameter evenly distributed holes immediately below the draft box. A small amount of secondary air was added to the bottom of the four annular sections. Finally, air was fed to the top of the bed through a tube of diameter 10 mm (with 26-1 mm holes) to mimic oxidation air in the reactor.

Air flow to the distributors was measured by rotameters. Pressure transducers were connected to impulse lines to monitor the system, including each channel in the draft box, annulus and freeboard region. Pressure data were recorded at both low frequency (<1 Hz) to provide steady state data and at high frequency (48 Hz) to determine pressure fluctuations. Solids circulation was measured by averaging visually recorded downward velocities in each of the four annular quadrants.

The 12th International Conference on Fluidization - New Horizons in Fluidization Engineering, Art. 63 [2007]

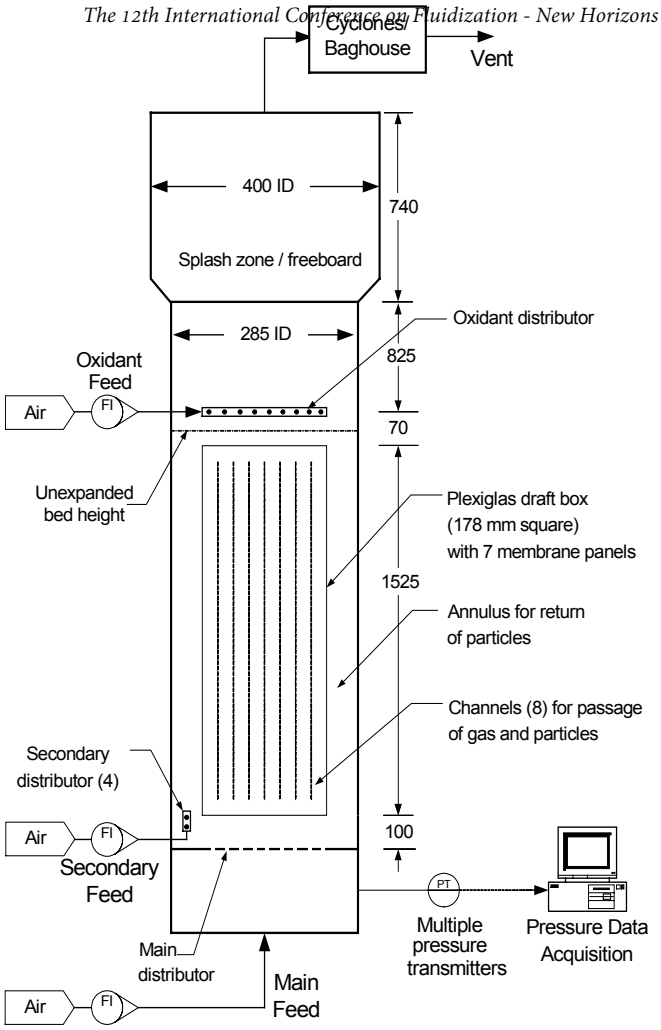

Figure 2: Unit schematic (dimensions in mm)

Figure 3 presents a plan view of the cold model. The seven panels within the draft box were removable to allow three different membrane panels geometries to be tested: Impervious (solid), vertically-slotted and horizontally-slotted (Figure 4, gray areas are open to flow). Although the solid panel has the largest area, and thus potential higher H_2 flux, there was a concern that slots would be required to prevent flow instability. The two slotted panels allow communication of gas and solids between the flow channels. The horizontally slotted panel (C) most closely represents the membrane layout used in the pilot reactor.

EXPERIMENT RESULTS

Solids Circulation

A series of experiments were carried out using the three panels described above. The impervious panels were tested first, followed by the horizontally-slotted, and finally vertically-slotted panels. All other system components remained unchanged for the tests. The main experimental variables were flow of main and secondary air.

The column operated very smoothly. As soon as the main air flow was started, gas flowed up the reactor core, and solids started to circulate up the core and down the annulus. No net upward flow of solids in the annular quadrants was observable for the range of column flows investigated. No significant bypassing of the main airflow to the annular regions could be observed for the range of conditions tested.

Circulation of solids improved significantly once a small flow of air was introduced to the bottom of the annular regions through the secondary distributor. No bubbles were noted in the annular regions until the secondary air flow reached about 10 SLM (0.6 Nm^3/h). Assuming a uniform distribution of gas, this corresponds to a superficial gas velocity in the annular region of 0.005 m/s, roughly double the measured U_{mf} for the FCC particles. Periodic bubbles were noted when the secondary air flow was increased to 20 SLM (1.2 Nm^3/h), and more significant gas flow up the annulus was noted at 30 SLM (1.8 Nm^3/h). Upward bubble movement in the annulus was hindered by downflow of solids, leading to occasional stagnation and bubble

flattening. No downward bubble flow in the annulus was observed. There was very significant bubbling at a secondary air flow of 40 SLM (2.4 Nm^3/h), but solids movement was still downward in all quadrants.

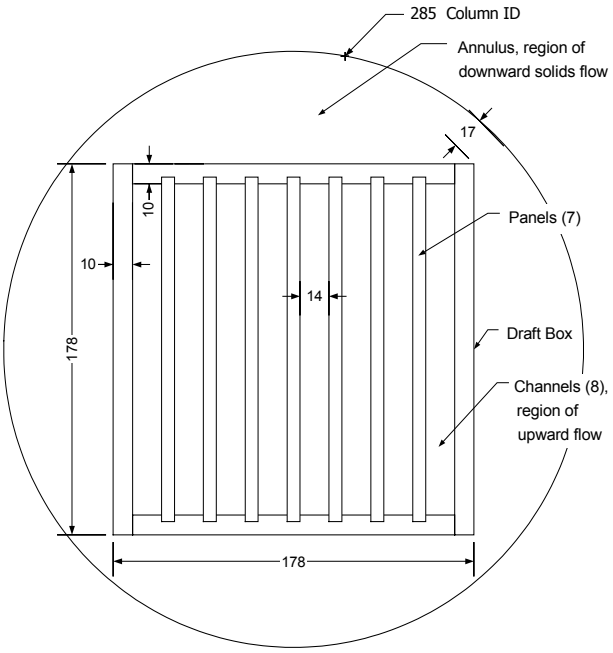

Figure 3: Cold model plan (dimensions in mm)

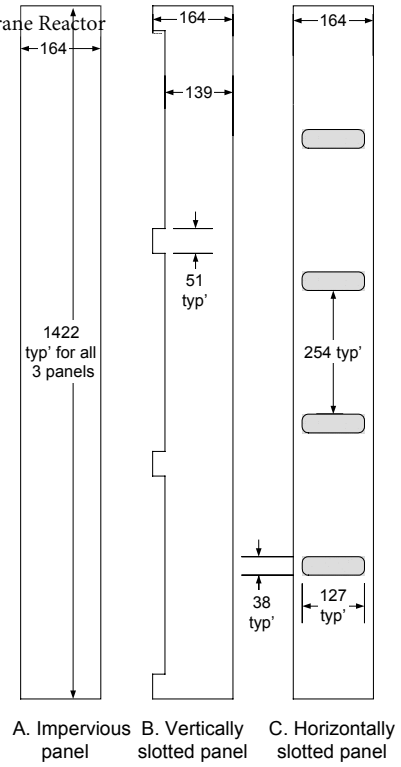

Figure 4: Membrane panel types (dimensions in mm)

Large variations in the pressure signals in the core channels were noted with the impervious membrane panels. It was apparent that these panels lead to unstable flow within the core draft box. Some channels had much higher solids hold-up, or perhaps were periodically plugged, compared to neighboring channels. Evidently, there is instability in the two-phase flow, with equal pressure drop through the parallel paths achievable by having a high gas velocity accompanied by a high voidages, or lower gas velocity / lower voidages, as reported by Bolthrunis et al. (10). No such behavior was detected with either the vertically slotted or horizontally slotted panels, where gas and solids were able to exchange between adjacent flow channels.

Downward solids velocity in the annular region is plotted as a function of main and secondary air flow for the vertically-slotted panels in Figure 5. The solids circulation rate increased approximately linearly with the main air flow until 500 SLM, at which point it leveled off. Doubling the secondary air flow from 10 to 20 SLM significantly increased solids circulation. Increasing the secondary air flow beyond 20 SLM did not change the solids circulation. Similar patterns were found with the impervious panels and the horizontally-slotted panels. The measured solids circulation rates for the three different solids panels at secondary air flow of 20 SLM are presented in Figure 6. The vertically slotted panels exhibited slightly higher circulation than the other two panel geometries for the range of conditions investigated.

The 12th International Conference on Fluidization - New Horizons in Fluidization Engineering, Art. 63 [2007]

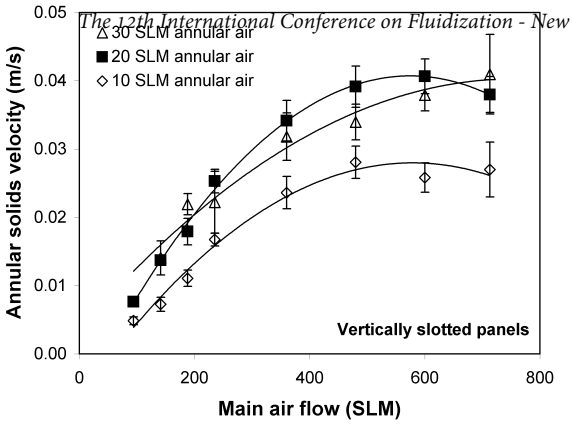

Figure 5: Downward solids velocity in the annulus with vertically-slotted panels as a function of main and secondary air flow (Bars show 95% confidence intervals)

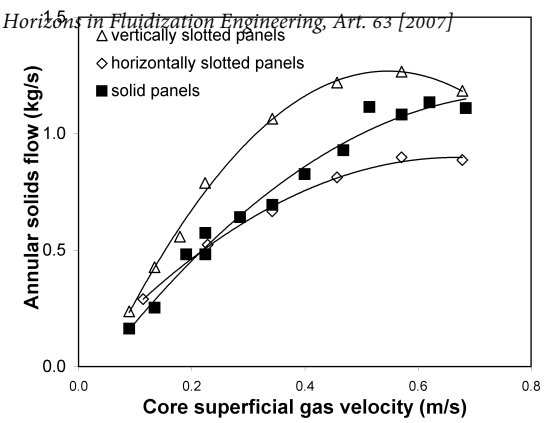

Figure 6: Average solids internal circulation rate with a secondary air flow of 20 SLM for the three panel geometries

Helium Gas Tracing

Steady-state gas movement within the bed was studied using helium as a tracer gas. A known flow of helium was added to the oxidant air flow. Gas samples were then withdrawn through a thermal conductivity detector (TCD) to determine the helium concentration at various points within the bed. Notable findings include:

- The measured helium concentration in the annulus (mid-height) was much higher than in the core, typically close to the He concentration at the column exit. This is expected, as the gas dragged down by the annular solids originates from the well-mixed zone in the upper column.
- Only ~10% of the helium in the oxidant air supply was circulated to the core.
- From the air flow to the column and the average He concentrations in the annulus and core, the amount of gas dragged down by the annular solids circulation was estimated. The solids circulation rate could then be estimated assuming a gas velocity of $U_{mf} / \varepsilon_{mf}$ relative to the particle in the annulus. Values estimated in this manner were within ±30% of those measured by visual observations.

DISCUSSION

The cold model testing clearly showed that impervious membrane panels within the draft box led to poor gas-solid distribution among the flow channels. Slotted communicating panels greatly improved the uniformity of gas and solids flow within the core, and are thus preferred in the ICFBMR design.

Solids circulation increased significantly when the annular gas flow increased from 10 to 20 SLM, but did not change significantly when annular flows increased beyond 20 SLM. Clearly the flow of particles down the annulus and in the return channel at the bottom, restricted solids flow at the lower gas flow. Increased bubbling near the bottom of the annular quadrants likely increased the mobility of solids as they turned inwards to enter the core. The extra annular air may have also helped to prevent local defluidization at various points in the annulus.

A consistent relationship was exhibited between solids circulation and core superficial velocity for all panels. For a given annular air gas flow, solids circulation increased nearly linearly with core gas superficial velocity up to ~0.3 m/s, after which it tended to level out. In a conventionally bubbling fluidized bed, solids are moved vertically within the bed in the wakes of rising bubbles. At core superficial velocities below 0.3 m/s, it is likely that the fluidization is in the bubbling flow regime, with the wake fraction relatively constant. For most testing in the cold model, $U_{core} >> U_{mf}$, so the circulation rate is therefore approximately proportional to U_{core}. It is further postulated that as the core superficial gas velocity increases above ~0.3 m/s, a gradual transition to turbulent fluidization occurs. Near-spherical bubbles are then increasingly replaced by streaking voids and the carrying capacity of the rising gas levels off.

The solids circulation correlation for the vertically slotted panels in Figure 6 was transformed to a solids circulation flux and scaled up to reforming conditions using the dimensionless group $G_{p,core} / \rho_p U_{core}$. The data were then incorporated into a HYSYS simulation of the ICFBMR producing 50 Nm^3/h of H_2.

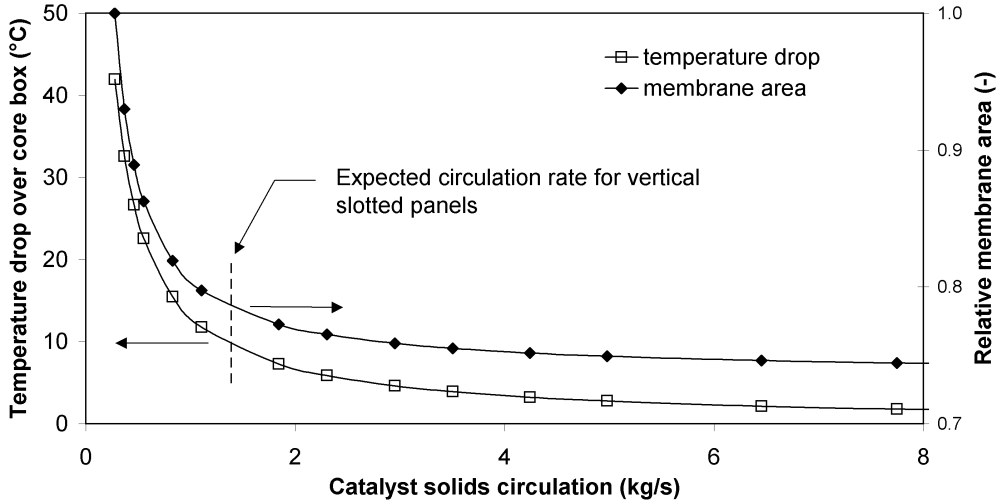

Figure 7: Effect of solids circulation on the core reactor temperature drop and relative membrane area. Conditions: 50 Nm^3/h H_2, steam:carbon molar ratio = 3, methane feed = 25 Nm^3/h, reactor pressure 1,500 kPa, feeds preheated to 650°C

At low solids circulation rates, less heat is circulated to the core, leading to a significant temperature gradient in the reactor core due to the endothermic heat of reaction. This reduces the H_2 flux due to lower membrane temperatures and lower equilibrium conversions, requiring more membrane area to achieve the unit capacity of 50 Nm^3/h. This effect is highlighted on the secondary axis in Figure 7. The experimental data indicate that the expected solids circulation rate for this geometry maintains the temperature drop in the core to an acceptable 10°C.

Pd-based membranes typically used for reactor applications are 20 to 75 μm thick. At this thickness, membrane characteristics tend to dominate reactor performance. Previous FBMR modeling studies (including Adris et al., 11) suggest that the catalyst holdup at the circulation rates discussed here are more than adequate to support reforming. Other hydrodynamic parameters, such as gas bypassing and gas mass transfer, have also been estimated to be of secondary importance. Circulating

fluidized bed membrane reformers have the potential to be applied to sorption-enhanced reforming in order to produce a CO_2-rich stream for sequestration (Prasad and Elnashaie, 12). A CO_2-absorbent such as limestone can be added to the bed to capture CO_2 from the reforming section and release the CO_2 in the return annulus.

CONCLUSIONS

Cold model testing of the ICFBMR geometry confirmed that an internally circulating fluidized bed is suitable for small-scale reforming from a hydrodynamic perspective. A number of specific design aspects warrant further study, including distributor design and reduction of the annular area.

ACKNOWLEDGMENTS

Support from Membrane Reactor Technologies Ltd. and the Natural Sciences and Engineering Research Council of Canada (NSERC) is gratefully acknowledged.

NOTATION

g	Acceleration due to gravity (9.81) [m/s^2]
$G_{p,core}$	Mass flux of solids up the ICFBMR core based on open area [kg/s m^2]
U_{core}	Superficial gas velocity in the reactor core based on area open to flow [m/s]
U_{mf}	Superficial gas velocity at minimum fluidization [m/s]
ε_{mf}	Bed voidage at minimum fluidization [-]
ρ_f	Gas density [kg/m^3]
ρ_p	Particle density [kg/m^3]

REFERENCES

1 Paglieri, S.N., Way, J.D., “Innovations in Palladium Membrane Research”, Separation and Purification Methods, 31(1), 1-169 (2002).
2 Uemiya, S., “Brief review of steam reforming using a metal membrane reactor”, Topics in Catalysis, 29, 79-84 (2004).
3 Adris, A.M., Lim, C.J., Grace, J.R., “The fluidized bed membrane reactor system: A pilot scale experimental study”, Chem. Eng. Sci., 49, 5833-5843 (1994).
4 Grace, J.R., Lim, C.J., Adris, A.M., Xie, D., Boyd, D.A., Wolfs, W.M., Brereton, C.M.H., US Patent Application No. 20050036940 (2006).
5 Boyd, T., Grace, J.R., Lim, C.J., Adris, A.M, “H_2 from an internally circulating fluidized bed membrane reactor”, Int. J. Chem. Reactor Eng., 3. A58, 2005.
6 Roy, S., Pruden, B., Adris, A.M., Grace, J.R., Lim, C.J., “Fluidized bed steam methane reforming with O_2 Input”, Chem. Eng. Sci., 54, 2095-2102 (1999).
7 Song, B.H., Kim, Y.T., Sang, D.K., “Circulation of solids and gas bypassing in an internally circulating fluidized bed with a draft tube”, Chem. Eng. Jour., 68, 115-122 (1997).
8 Milne, B.J., Berruti, F., Behre, L.A., de Bruijn, T.J.W., “The internally circulating fluidized bed: A novel solution to gas bypassing in spouted beds”, CJChE, 70, 910-915 (1992).
9 Glickman, L.R., Hyre, M., Woloshun, K., “Simplified scaling relationships for fluidized beds”, Powder Technology, 77, 177-199 (1993).
10 Bolthrunis, C.O., Silverman, R.W., Ferrari, D.C, “The rocky road to commercialization: breakthroughs and challenges in the commercialization of fluidized bed reactors”, Fluidization XI (2004).
11 Adris, A.M., Lim, C.J., Grace, J.R., “The fluidized bed membrane reactor for steam methane reforming: model verification and parametric study”, Chem. Eng. Sci., 52, 1609-1622 (1997).
12 Prasad, P., Elnashaie, S.S.E.H., “Novel circulating fluidized-bed membrane reformer using carbon dioxide sequestration”, Ind. Eng. Chem. Res., Vol. 43, 494-501 (2004).